Chaos, Solitons & Fractals: X 3 (2019) 100019

Contents lists available at ScienceDirect

Chaos, Solitons & Fractals: X

journal homepage: www.elsevier.com/locate/csfx

The size of Mandelbrot bulbs

A.C. Fowler [a,b,*], M.J. McGuinness [c]

[a] MACSI, University of Limerick, Limerick, Ireland
[b] OCIAM, Mathematical Institute, University of Oxford, Oxford, UK
[c] School of Mathematics and Statistics, Victoria University of Wellington, Wellington, New Zealand

ARTICLE INFO

Article history:
Received 5 August 2019
Revised 11 November 2019
Accepted 6 December 2019
Available online 9 December 2019

Keywords:
Mandelbrot set
Mandelbrot bulbs

ABSTRACT

We provide an analytic estimate for the size of the bulbs adjoining the main cardioid of the Mandelbrot set. The bulbs are approximate circles, and are associated with the stability regions in the complex parameter μ-space of period-q orbits of the underlying map $z \to z^2 - \mu$. For the (p, q) orbit with winding number p/q, the associated stability bulb is an approximate circle with radius $\frac{1}{q^2} \sin \frac{\pi p}{q}$.

1. Introduction

The Mandelbrot set, as shown in Fig. 1, is defined as the set of points μ in the complex plane for which the origin $z = 0$ is *not* mapped to ∞ under iteration of the quadratic map

$$z \to z^2 - \mu. \tag{1.1}$$

One way to compute it is to use the escape time algorithm. For a point μ in the complex plane, we associate an integer $N(R, \mu)$, which is the number of iterates of the map (starting with $z = 0$) which are required so that $|z| > R$. The Mandelbrot set is the set of values for which $N = \infty$ for sufficiently large R. In practice one takes R as fixed and large, and presumes $N = \infty$ if $N > N_\infty$, where N_∞ is suitably large.

The Mandelbrot set consists of the black points in Fig. 1. Commonly one colours each pixel according to its value of N. The coloured hues in Fig. 1 are thus associated with points which do diverge to ∞. For artistic reasons, the colour scale is highly nonlinear.

The map (1.1) has an infinite number of periodic orbits, and indeed these are simply counted. A q-periodic orbit is a fixed point of the map $z \to z_q$, where z_q is the qth iterate of (1.1) and is a polynomial in z of degree 2^q, thus having 2^q roots; these correspond to period-r orbits, where the set of r values contains the factors of q. We can thus count the number of period-q orbits by successive evaluation for increasing q. For example, there are two fixed points ($q = 1$, $2^q = 2$). For $q = 2$, there are $2^2 = 4$ roots of $z_2 = z$, but two of these are the fixed points, and the other two provide one period-2 orbit, since a root z of period two implies z_1 is also a root corresponding to the same orbit.

Likewise, we have eight roots of period three, and thus $(2^3 - 2)/3 = 2$ period-3 orbits. For $q = 4$, there are sixteen roots, four of which are the fixed points and the period-2 orbit, so there are three period-4 orbits; for $q = 5$, there are six period-5 orbits; and so on. (When q is prime, the necessary fact that q divides $2^q - 2$ is a consequence of Fermat's little theorem.)

Each of these orbits has a region or regions in μ-space where it is stable, and these regions provide the obvious distinct regions of the Mandelbrot set: distinct, as it is known that the map has no more than one stable periodic orbit. Most of the regions appear to be approximately circular, except for the largest region, which is a cardioid, and is the stability region for one of the fixed points.

In more detail, the fixed points of the map are

$$z^{\pm} = \tfrac{1}{2} \pm \left(\mu + \tfrac{1}{4}\right)^{1/2}. \tag{1.2}$$

The stability of the fixed point is given by the criterion that the modulus of the derivative of the right hand side of (1.1) is less than one. If we define the positive square root $(1 + 4\mu)^{1/2}$ to have positive real part, then z^+ is always unstable, and the stability of z^- requires

$$|1 - (1 + 4\mu)^{1/2}| < 1. \tag{1.3}$$

Solving for the boundary, we obtain $\mu + \frac{1}{4} = e^{i\theta} \cos^2 \frac{1}{2}\theta$, where θ is the polar angle with respect to $\mu = -\frac{1}{4}$, and thus in the same polar coordinates,

$$r = \cos^2 \tfrac{1}{2}\theta, \tag{1.4}$$

* Corresponding author.
E-mail address: andrew.fowler@ul.ie (A.C. Fowler).

https://doi.org/10.1016/j.csfx.2019.100019

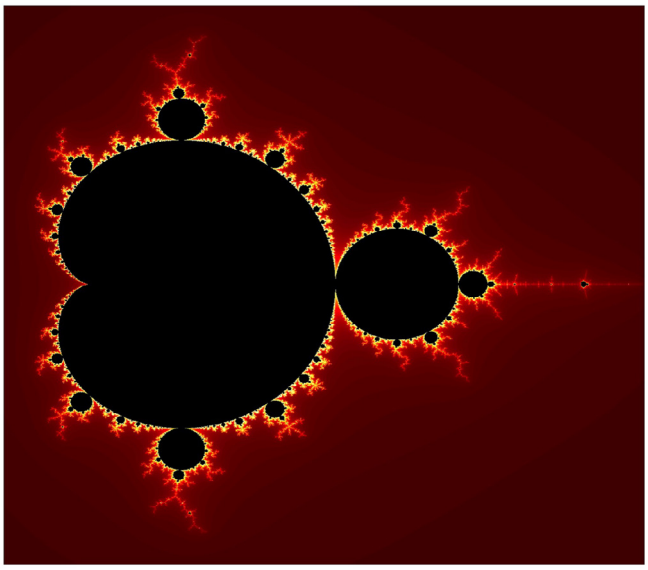

Fig. 1. The Mandelbrot set.

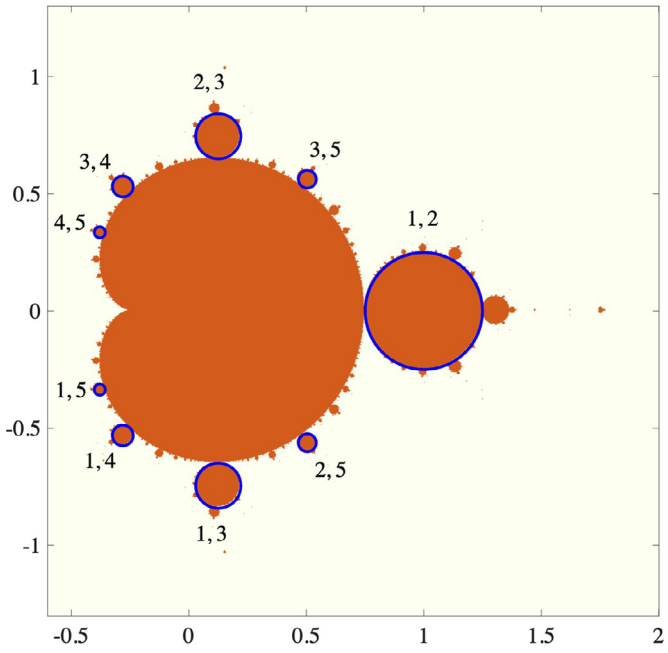

Fig. 2. The Mandelbrot set, overlain with the main cardioid bulbs of periods 2,3,4,5, with an approximate circular form (in blue) of radius a_q from (1.8). The number pairs by each bulb give the values of p and q at the corresponding tangential resonance; see (1.7). (For interpretation of the references to colour in this figure legend, the reader is referred to the web version of this article.)

which is the equation of a *cardioid*. This is the smooth contour of the large bulb of the figure, with the origin taken at the cusp of the cardioid.

Similarly, the circle to its right is the stability region for the period two cycle, and the smaller one to its right is that for a period four cycle. The process carries on as for the Feigenbaum sequence, yielding smaller and smaller regions of stability. Further out past the limiting value of $\mu_\infty \approx 1.40\ldots$, there are other small regions, the most noticeable of which corresponds to the period three window at $\mu \approx 1.75$.

We can assess the stability of the period-2 cycle in the same way as above. The two values $\{z_+, z_-\}$ of the 2-cycle satisfy the quartic equation

$$z = (z^2 - \mu)^2 - \mu; \tag{1.5}$$

however, two of the roots of this are the fixed points, so the quartic can be factorised, and we find that

$$z_\pm = -\tfrac{1}{2} \pm (\mu - \tfrac{3}{4})^{1/2}. \tag{1.6}$$

The stability region of the period-2 cycle is $|4z_+z_-| < 1$, and this is the circle $|\mu - 1| < \frac{1}{4}$. This is the bulb to the right of the cardioid in Fig. 1.

Many other bulbs can be seen round the periphery; those touching the main cardioid correspond to stability regions for period q cycles having a rotation number of $\frac{p}{q}$ (we may take p and q to be relatively prime), and they touch the cardioid at

$$(1 + 4\mu)^{1/2} - 1 = e^{i\alpha}, \quad \alpha = \pi\left(\frac{2p}{q} - 1\right). \tag{1.7}$$

The large period-2 cycle stability bulb to the right of the cardioid corresponds to $p = 1,\ q = 2$; the bulbs at the bottom and top (respectively) of the cardioid represent period-3 cycle stability boundaries, $p = 1, 2,\ q = 3$; and so on. It is evident that there is a good deal of self-similarity in the figure, and exotic features can be traced down to indefinitely small scales.

In this paper we are concerned with the shape and size of the main cardoid bulbs. Evidently they are approximate circles which are tangent to the cardioid, and Fig. 2 shows that the radius of the (p, q) bulb is well approximated by

$$a_q = \frac{1}{q^2} \sin\frac{\pi p}{q}. \tag{1.8}$$

Our intention is to explain this observation.

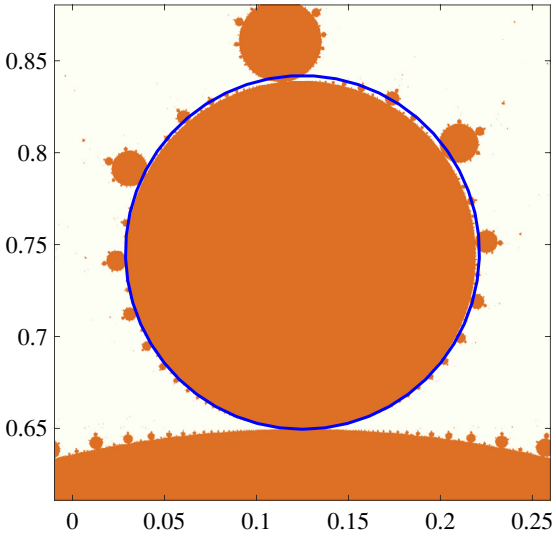

Fig. 3. A close-up of the (2,3) bulb, together with its analytic approximate shape as in (2.6).

The Mandelbrot set has been studied for many years (see for example [2,4–7]), and the geometry of the bulbs has been a subject of continuing interest, but the estimate in (1.8) appears not to have been demonstrated explicitly, other than as a numerical observation; see, for example [10], whose result (the Mandelbrot n^2 conjecture) is discussed further in Section 5. There has been some interest in computing the area of the Mandelbrot set (e. g., [1]), but apparently without concern for the actual bulb shapes or sizes.

It should be pointed out that the bulbs' apparent circular shape is indeed only approximate, as is shown in Fig. 3, where the 2/3 bulb is shown in close-up. The approximate formula (2.6) which we derive below describes a circle whose boundary is shown in blue: it is close but not exact.

2. Bulb bifurcations

We begin with some geometry. On the main cardioid

$$r = \cos^2 \tfrac{1}{2}\theta, \quad \mu + \tfrac{1}{4} = re^{i\theta}, \tag{2.1}$$

the angle of the tangent at polar angle θ follows from

$$\tan\psi = \frac{dy}{dx} = \frac{(r(\theta)\sin\theta)'}{(r(\theta)\cos\theta)'}, \tag{2.2}$$

and evaluating this we find

$$\psi = \tfrac{3}{2}\theta - \tfrac{1}{2}\pi. \tag{2.3}$$

The two bulbs at the top and bottom of the cardioid have $\psi = 0$ and $-\pi$, corresponding to $\theta = \pm\frac{1}{3}\pi$, and thus from (1.7) $\frac{p}{q} = \frac{2}{3}, \frac{1}{3}$: these are the period-3 stability bulbs. Similarly, the period-4 stability bulbs associated with $\frac{p}{q} = \frac{3}{4}, \frac{1}{4}$ are located at $\theta = \pm\frac{1}{2}\pi$, immediately above and below the cusp of the cardioid.

Next, we write the map in terms of a perturbation of the fixed point $z^- = z^*$ when $\mu = \mu^*$ is on the cardioid and $\theta = \alpha$ given in (1.7). Define

$$z = z^* + \zeta, \quad \mu = \mu^* + \Delta, \quad \mu^* = -\tfrac{1}{4} + e^{i\alpha}\cos^2\tfrac{1}{2}\alpha, \tag{2.4}$$

so that the map is transformed to

$$\zeta \to s\zeta + \zeta^2 - \Delta, \quad s = -e^{i\alpha} = \exp\left(\frac{2\pi i p}{q}\right). \tag{2.5}$$

The (p, q) bulb sprouts from $\mu = \mu^*$, where the fixed point z^- loses stability, and a stable period-q orbit is born.

We will show that the stability region for this period-q orbit is the approximate circle

$$\left|\Delta e^{-i\psi} - ia_q\right| < a_q, \quad a_q = \frac{1}{q^2}\sin\frac{\pi p}{q}. \tag{2.6}$$

Note that the complex variable $\Delta e^{-i\psi}$ has its real axis along the tangent to the cardioid, so that the circles are external and tangent to it, as can be seen in Fig. 1.

3. A failed approximation method

The period-q orbits of (2.5) exchange stability with the fixed point when $\Delta = 0$. For $\Delta = 0$ and $\zeta \ll 1$, the linearised map $\zeta \to s\zeta$ has a (degenerate) family of q-periodic solutions, so it is natural to seek perturbation methods when $\Delta \ll 1$. In this section we attempt to do this; the method is non-standard, both because we are attempting to analyse a weakly non-linear *difference* equation, and also because the result (2.6) suggests that the small value of Δ should be related to large values of q. As we shall see, we are unable to provide a satisfactory solution method, partly on this account.

Let the rth iterate of (2.5) be ζ_r, so that

$$\zeta_{r+1} = s\zeta_r + \zeta_r^2 - \Delta, \quad s = \exp\left(\frac{2\pi i p}{q}\right), \quad \zeta_0 = \zeta, \tag{3.1}$$

and assume that ζ_r and Δ are small. If we define

$$D_\pm(\zeta) = \zeta^2 \pm (1-s)\zeta - \Delta, \tag{3.2}$$

then the fixed points of the map correspond to the solutions of $D_- = 0$. We assume ζ is not a fixed point of the map, and by defining

$$\zeta_r = \zeta + D_- A_r, \tag{3.3}$$

it follows that

$$A_{r+1} = 1 + sA_r + 2\zeta A_r + D_- A_r^2, \quad A_0 = 0, \tag{3.4}$$

and q-periodic orbits have $A_q = 0$. The approximate solution (with $\zeta, D_- \ll 1$) is

$$A_r = \frac{1-s^r}{1-s}, \tag{3.5}$$

and this represents a (neutrally stable) period-q orbit.

Next we define

$$A_r = \frac{1-s^r u_r}{1-s}, \tag{3.6}$$

from which it follows that

$$u_{r+1} = u_r - \frac{D_+}{s(1-s)}\frac{1}{s^r} + \frac{2(\zeta^2-\Delta)u_r}{s(1-s)} - \frac{D_- u_r^2}{s(1-s)}s^r, \quad u_0 = 1, \tag{3.7}$$

and a period-q ($q > 1$) orbit corresponds to having $u_q = 1$.

In a naïve approximation, we may note that for small ζ and Δ, $u_r \approx 1$, so that

$$u_{r+1} \approx u_r - \frac{D_+}{s(1-s)}\frac{1}{s^r} + \frac{2(\zeta^2-\Delta)}{s(1-s)} - \frac{D_-}{s(1-s)}s^r, \quad u_0 = 1, \tag{3.8}$$

of which the solution is

$$u_r \approx 1 - \frac{D_+}{s(1-s)}\left(\frac{1-s^{-r}}{1-s^{-1}}\right) + \frac{2(\zeta^2-\Delta)r}{s(1-s)} - \frac{D_-}{s(1-s)}\left(\frac{1-s^r}{1-s}\right). \tag{3.9}$$

It follows that

$$u_q \approx 1 + \frac{2q(\zeta^2-\Delta)}{s(1-s)}, \tag{3.10}$$

and thus that there is a period-q orbit through $\zeta \approx \pm\sqrt{\Delta}$. The resulting region of stability is the bulb defined approximately by $|\zeta_q'(\zeta)| < 1$, and using (3.3), (3.6) and (3.10), this leads to the definition

$$\left|\Delta e^{-i\psi} - ia\right| < a, \quad a = \frac{1}{2q}\sin\frac{\pi p}{q}, \tag{3.11}$$

where we use the fact that

$$s(1-s) = -2ie^{i\psi}\sin\frac{\pi p}{q}. \tag{3.12}$$

This result is exact for $q = 2$, but incorrect for $q > 2$. Indeed the fact that there are two fixed points for ζ tells us we are only dealing with period-2 orbits, as period-q orbits would have q fixed points. What is wrong? The approximation (3.9) can only be applicable if $q\Delta \ll 1$, but the result in (3.11) suggests that $q\Delta \sim 1$, so that the approximation breaks down.

3.1. Multiple scales

The method described above is somewhat simple, but can be made more methodical using the *method of multiple scales for difference equations* (see, for example, Hoppensteadt and Miranker [9]). Specifically, if we write

$$\Delta = \varepsilon^2, \quad \zeta = \varepsilon Z, \quad R = \varepsilon r, \quad u_r = U(r,R) \equiv U_r(R), \tag{3.13}$$

and presume that the dependence on R is continuous, so that

$$u_{r+1} = U_r(R) + \varepsilon U_r'(R) + \ldots, \tag{3.14}$$

where the prime denotes differentiation with respect to R, then with

$$U \sim U^{(0)} + \varepsilon U^{(1)} + \ldots, \tag{3.15}$$

one can show by equating successive powers of ε that

$$U_r^{(0)} = U_0(R), \quad U_r^{(1)} = U_1(R) + \frac{Z}{s}\left[\frac{1-s^r}{1-s} - \frac{1-s^{-r}}{1-s^{-1}}\right], \tag{3.16}$$

and the functions U_0 and U_1 are determined by the requirement that secular terms be suppressed (so that the solutions are q-periodic). It then follows that $U_0 \equiv 1$ and, by removing secular terms at $O(\varepsilon^2)$, that

$$U_1 = \frac{-2R}{s(1-s)}, \tag{3.17}$$

but this does not seem to lead anywhere. Part of the problem is that it is unclear how ζ should be related to Δ, and as we shall see, the assumption in (3.13) that $\zeta \sim \Delta^{1/2}$ is in fact only appropriate if $q = 2$.

4. Derivation of the bulb radius

To elucidate the issue, we look at explicit iterates of the map (3.1), using (3.4). We find

$$A_0 = 0, \quad A_1 = 1, A_2 = D_- + (1 + s + 2\zeta),$$
$$A_3 = D_-^3 + 2(1 + s + 2\zeta)D_-^2 + \{s + 2\zeta + (1 + s + 2\zeta)^2\}D_- + (s + 2\zeta)(1 + s + 2\zeta) + 1, \tag{4.1}$$

and so on. Since $D_- = 0$ at the fixed points of the map, a period q orbit is one for which $A_q = 0$ (and $A_r \neq 0$ for $1 \le r < q$).

Consider first the $p = 1$, $q = 2$ resonance for which $s = -1$ and a period 2 orbit bifurcates at $\Delta = 0$. In this case $D_- = \zeta^2 - 2\zeta - \Delta$, and thus $A_2 = \zeta^2 - \Delta$; this is exact, and is in fact identical to the approximate result in (3.10) (given that $s = -1$). Thus the stability result in (2.6) is exact for $q = 2$.

Now let us see what happens for $q = 3$. In this case we take $s = \exp(\pm 2\pi i/3)$, and thus $s^3 = 1$, $1 + s + s^2 = 0$. Using these, we find

$$A_3(D_-, \zeta) = D_-^3 + 2(1 + s + 2\zeta)D_-^2 + 2\{s + (3 + 2s)\zeta + 2\zeta^2\}D_- + 2\zeta(1 + 2s + 2\zeta). \tag{4.2}$$

We define

$$D(\zeta) = \zeta^2 - (1 - s)\zeta, \tag{4.3}$$

so that $D_- = D - \Delta$, and we want to find the roots of $A_3 = 0$ for small Δ. Evidently these are close to the roots of $P_3(\zeta) \equiv A_3[D(\zeta), \zeta]$, and simplifying this using (4.2), we find

$$P_3(\zeta) = \zeta^3[\zeta^3 + (1 + 3s)\zeta^2 - (2 - s)\zeta - (3 + 2s)]. \tag{4.4}$$

For small Δ, we then have

$$A_3(D_-, \zeta) = P_3(\zeta) - \Delta\frac{\partial A_3}{\partial D} + \dots. \tag{4.5}$$

The map $\zeta \to \zeta_3$ is an eighth-degree polynomial. It has two fixed points corresponding to the fixed points of the map (2.5), and the other six roots, which are those of A_3, correspond to the two period 3 orbits. It is evident from (4.4) that the period 3 orbit of concern in the bifurcation is that corresponding to the three roots near zero. From (4.2),

$$\frac{\partial A_3}{\partial D} = 2s + O(\zeta), \tag{4.6}$$

and thus (4.5) gives

$$A_3 = c_3\zeta^3 - b_3\Delta + \dots, \quad c_3 = -(3 + 2s), \quad b_3 = 2s, \tag{4.7}$$

so that the correct approximation for the roots has $\zeta \sim \Delta^{1/3}$, in distinction to (3.13).

This provides a clue as to what we should predict: for period q orbits, we expect that if $s^q = 1$, $1 + s + s^2 + \dots + s^{q-1} = 0$, then

$$A_q = c_q\zeta^q - b_q\Delta + \dots; \tag{4.8}$$

substituting this into (3.3) and calculating the approximate value of $\zeta_q'(\zeta)$, we find the stability condition as in (2.6), with the value of a_q for period q orbits being

$$a_q = \frac{1}{Q}\sin\frac{\pi p}{q}, \quad Q = -\tfrac{1}{2}qb_qs(1 - s)^2, \tag{4.9}$$

where we again make use of the formula $s(1 - s) = -2ie^{i\psi}\sin\frac{\pi p}{q}$. For $q = 2$ and $q = 3$, we regain (2.6). The task is now to demonstrate that (4.8) applies for any q, and that $Q = q^2$ in (4.9). A similar result to (4.8) is present in the work of [3], (proposition 8).

4.1. Expansion for A_q

We write the map (3.4) in the form

$$A_{r+1} = 1 + \lambda A_r + (D - \Delta)A_r^2, \quad A_0 = 0, \tag{4.10}$$

where

$$\lambda(\zeta) = s + 2\zeta, \quad D(\zeta) = \zeta^2 - (1 - s)\zeta. \tag{4.11}$$

The solution of (4.10) is a function $A_r(D - \Delta, \lambda)$, and a period-q orbit corresponds to a value of ζ for which $A_q[D(\zeta) - \Delta, \lambda(\zeta)] = 0$. When $\Delta \ll 1$, we have

$$A_q[D(\zeta) - \Delta, \lambda(\zeta)] = A_q[D(\zeta), \lambda(\zeta)] - \Delta\frac{\partial A_q}{\partial D}[D(\zeta), \lambda(\zeta)] + \dots, \tag{4.12}$$

in analogy to (4.5), and we aim to calculate these two coefficients.

Putting $\Delta = 0$, (4.10) becomes

$$A_{r+1} = 1 + \lambda A_r + DA_r^2, \quad A_0 = 0, \tag{4.13}$$

and we expand as a power series

$$A_r = a_0^{(r)}(\lambda) + a_1^{(r)}(\lambda)D + a_2^{(r)}(\lambda)D^2 + \dots, \tag{4.14}$$

whose form can be ascertained by induction. Substituting into (4.13) and equating powers of D, we find

$$a_0^{(r+1)} = 1 + \lambda a_0^{(r)}, \quad a_0^{(0)} = 0,$$
$$a_1^{(r+1)} = \lambda a_1^{(r)} + a_0^{(r)2}, \quad a_1^{(0)} = 0, \tag{4.15}$$

etc., for which the solutions are

$$a_0^{(r)} = \frac{1 - \lambda^r}{1 - \lambda}, \quad a_1^{(r)} = \frac{\lambda + (1 - \lambda)(1 - 2r)\lambda^r - \lambda^{2r}}{\lambda(1 - \lambda)^3}. \tag{4.16}$$

Putting $r = q$ and expanding for small ζ, we find

$$\frac{\partial A_q}{\partial D}[D(\zeta), \lambda(\zeta)] = b_q + O(\zeta), \quad b_q = -\frac{2q}{s(1 - s)^2}. \tag{4.17}$$

Note that with Q defined as in (4.9), this gives $Q = q^2$.

4.1.1. Calculation of $A_q[D(\zeta), \lambda(\zeta)]$

Next we wish to calculate $A_q[D(\zeta), \lambda(\zeta)]$ in (4.12). This is a little more complicated. For this we return to the original map (3.1), but with $\Delta = 0$:

$$\zeta_{r+1} = s\zeta_r + \zeta_r^2, \quad \zeta_0 = \zeta; \tag{4.18}$$

note that the solution is

$$\zeta_r = \zeta + D(\zeta)A_r[D(\zeta), \lambda(\zeta)]. \tag{4.19}$$

We write the solution of (4.18) as a power series:

$$\zeta_r = a_{1,r}\zeta + \dots + a_{j,r}\zeta^j + \dots, \tag{4.20}$$

whose form is confirmed by induction. Computations of low order polynomials of this type have been constructed by Stephenson [11], 12] and Stephenson and Ridgway [13]. The initial conditions are

$$a_{1,0} = 1, \quad a_{j,0} = 0, \quad j > 1. \tag{4.21}$$

Expanding (4.18) and equating powers of ζ, we obtain

$$a_{1,r+1} = sa_{1,r}, \quad a_{1,0} = 1,$$
$$a_{2,r+1} = sa_{2,r} + a_{1,r}^2, \quad a_{2,0} = 0,$$
$$a_{3,r+1} = sa_{3,r} + 2a_{1,r}a_{2,r}, \quad a_{3,0} = 0,$$

$$\vdots$$

$$a_{j,r+1} = sa_{j,r} + \sum_{m=1}^{j-1} a_{m,r}a_{j-m,r}, \quad a_{j,0} = 0. \tag{4.22}$$

Solving these, we find sequentially that

$$a_{1,r} = s^r, \quad a_{2,r} = \frac{s^r - s^{2r}}{s - s^2}, \quad a_{3,r} = \frac{2}{s - s^2}\left[\frac{s^r - s^{2r}}{s - s^2} - \left(\frac{s^r - s^{3r}}{s - s^3}\right)\right]. \tag{4.23}$$

This suggests an *ansatz* that

$$a_{j,r} = \sum_{k=2}^{j} b_{jk}\left(\frac{s^r - s^{kr}}{s - s^k}\right), \quad j \geq 2. \tag{4.24}$$

Comparing this with (4.23), we see that

$$b_{22} = 1, \quad b_{32} = \frac{2}{s - s^2}, \quad b_{33} = -\frac{2}{s - s^2}. \tag{4.25}$$

Supposing (4.23) is true up to $j-1$, then for $j \geq 3$, (4.22) implies

$$a_{j,r+1} = sa_{j,r} + 2s^r \sum_{k=2}^{j-1} b_{j-1,k}\left(\frac{s^r - s^{kr}}{s - s^k}\right) + \sum_{m=2}^{j-2}\sum_{k=2}^{m}\sum_{l=2}^{j-m} b_{mk}b_{j-m,l}\left(\frac{s^r - s^{kr}}{s - s^k}\right)\left(\frac{s^r - s^{lr}}{s - s^l}\right). \tag{4.26}$$

On the right hand side of this expression the maximal value of n in terms s^{nr} is $n = j$, and therefore if $s^q = 1$, the inductive step to j will work providing $j \leq q$, since then there are no resonant terms $\propto s^r$ on the right hand side. Thus putting $r = q$ in (4.23) and (4.24), we find

$$a_{1,q} = 1, \quad a_{j,q} = 0, \quad j = 2, \ldots, q, \tag{4.27}$$

and thus

$$\zeta_q = \zeta + a_{q+1,q}\zeta^{q+1} + O(\zeta^{q+2}). \tag{4.28}$$

Note that due to (4.19), this implies that as $\zeta \to 0$,

$$A_q[D(\zeta), \lambda(\zeta)] = c_q\zeta^q + O(\zeta^{q+1}), \quad c_q = -\frac{a_{q+1,q}}{1 - s}. \tag{4.29}$$

Now although the *ansatz* (4.24) does not apply for $j = q + 1$, the Eq. (4.26) still determines $a_{q+1,r}$. In particular, determination of $a_{q+1,q}$ only requires the particular solution of (4.26) for the resonant terms $\propto s^r$ on the right hand side. Including these, we have

$$a_{q+1,r+1} = sa_{q+1,r} + s^r\left[\frac{2b_{qq}}{1 - s} + \sum_{m=2}^{q-1} \frac{b_{mm}b_{q+1-m,q+1-m}}{(s - s^m)(s - s^{q+1-m})}\right] + \ldots, \tag{4.30}$$

where the non-resonant terms are omitted, the point being that when $r = q$, their contributions all vanish. Solving this and putting $r = q$, we obtain

$$a_{q+1,q} = \left[\frac{2b_{qq}}{1 - s} + \sum_{m=2}^{q-1} \frac{b_{mm}b_{q+1-m,q+1-m}}{(s - s^m)(s - s^{q+1-m})}\right]\frac{q}{s}. \tag{4.31}$$

Now we return to the difference Eq. (4.26). Focussing on the coefficient b_{jj}, and noting that the solution of $a_{r+1} = sa_r + s^{kr}$ with $a_0 = 0$ is just $a_r = \dfrac{s^r - s^{kr}}{s - s^k}$, it follows that

$$b_{jj} = -\frac{2b_{j-1,j-1}}{s - s^{j-1}} + \sum_{m=2}^{j-2} \frac{b_{mm}b_{j-m,j-m}}{(s - s^m)(s - s^{j-m})}, \quad 3 \leq j \leq q. \tag{4.32}$$

Defining

$$C_j = \frac{b_{jj}}{s - s^j}, \tag{4.33}$$

we thus have

$$a_{q+1,q} = \left[-2C_q + \sum_{m=2}^{q-1} C_mC_{q+1-m}\right]\frac{q}{s}, \tag{4.34}$$

where

$$(s - s^j)C_j = -2C_{j-1} + \sum_{m=2}^{j-2} C_mC_{j-m}, \quad 3 \leq j \leq q, \quad C_2 = \frac{1}{s - s^2}. \tag{4.35}$$

As a curiosity, we derive a formal functional equation for the determination of C_m. If we define

$$f(x) = \sum_{2}^{\infty} C_m x^m, \tag{4.36}$$

it follows from summing (4.35) that

$$sf(x) - f(sx) = [f(x) - x]^2; \tag{4.37}$$

If we then define

$$g(x) = f(x) - x = \sum_{1}^{\infty} C_m x^m, \tag{4.38}$$

where we choose $C_1 = -1$, it follows that

$$sg(x) - g(sx) = g(x)^2. \tag{4.39}$$

It should be noted that if $s^q = 1$ for any q, then the infinite series (4.36) does not exist. Considered as a function $g(x, s)$, g is singular (in s) at any qth root of one, and thus in fact anywhere on the unit circle $|s| = 1$; we might surmise that it is analytic for $|s| < 1$, however. Luckily, explicit calculation of $a_{q+1,q}$ is not necessary for calculation of the bulb geometry.

4.1.2. The size of the bulbs

We now revert to the problem at hand. From (4.12), (4.17) and (4.29), the qth iterate for A_q is

$$A_q = c_q\zeta^q - b_q\Delta + O(\zeta^{q+1}, \Delta\zeta), \tag{4.40}$$

so that (4.9) is validated, and the value of b_q from (4.17) vindicates the value of a_q in (1.8). The only other item of interest is the calculation of the period-q orbits themselves. This requires the calculation of c_q, and thus (from (4.29)) $a_{q+1,q}$. Specifically,

$$c_q = -\frac{q}{s(1 - s)}\left[-2C_q + \sum_{m=2}^{q-1} C_mC_{q+1-m}\right], \tag{4.41}$$

where the coefficients C_j are calculated from (4.35); thus from (4.17) and (4.40), the bifurcating period-q orbit is approximately given by the q roots

$$\zeta \approx \left\{\frac{2\Delta}{(1 - s)\left[-2C_q + \sum_{m=2}^{q-1} C_mC_{q+1-m}\right]}\right\}^{1/q}. \tag{4.42}$$

5. Conclusions

To our knowledge, an estimate of the bulb radius of

$$a_q = \frac{1}{q^2}\sin\frac{\pi p}{q} \tag{5.1}$$

as given in (1.8), has not been directly demonstrated before, although its value can be found strewn across the internet, presumably based on numerical estimates. Here we have shown that it can

be predicted on a simple analytical basis in the limit that $\Delta \ll 1$, which is to say that the bulb radius is small.

A referee draws our attention to a result of [10], known as the Mandelbrot n^2 conjecture, and considers that our result is equivalent. The conjecture was proved by Guckenheimer and McGehee [8], but its relation to the present result is at the least opaque. Mandelbrot calls the bulbs 'atoms' with 'nuclei', and the bulb radius is the distance from the 'root' (in our case the point of tangency with the main cardioid) to the nucleus. The nucleus is defined as a point where 'the attractor of the corresponding [map] contains the critical point [$z = 0$]'; that is to say, where the period-q orbit is superstable. Why this should be at the centre of the approximately circular bulb is not clear, but supposing it to be the case, Mandelbrot then suggests (p. 222) that the radius of the bulbs in his set M_λ is numerically observed to be approximately $1/q^2$ (using our notation for the (p, q) bulb).

Mandelbrot considers his Mandelbrot set in two forms: as M_μ, associated with the mapping $z \to z^2 - \mu$, or as M_λ, associated with the mapping

$$Z \to F(Z) \equiv \lambda Z(1 - Z), \tag{5.2}$$

which can be obtained from the first map by writing $z = \frac{1}{2}\lambda - \lambda Z$, and

$$\mu = \tfrac{1}{4}\lambda^2 - \tfrac{1}{2}\lambda. \tag{5.3}$$

Thus to compare his numerical observation with our prediction (2.6), we need to write our result in terms of λ. Doing this, we find

$$\Delta e^{-i\psi} = e^{-\frac{3i\pi p}{q}}\left[\left(\frac{\lambda - 1}{2}\right)^2 + e^{\frac{2i\pi p}{q}} \sin^2 \frac{\pi p}{q}\right], \tag{5.4}$$

thus the root of an M_λ bulb is at ($\Delta = 0$)

$$\frac{\lambda - 1}{2} = \pm e^{\frac{i\pi p}{q}} \sin \frac{\pi p}{q}. \tag{5.5}$$

M_λ is symmetric about $\lambda = 1$, both horizontally and vertically, and the main cardioid of M_μ becomes the two primary bulbs $|\lambda| < 1$ and $|\lambda - 2| < 1$. In (5.5), the upper sign corresponds to the left primary bulb, and the lower sign corresponds to the right primary bulb. We define

$$\lambda = 1 \pm 2ie^{\frac{i\pi p}{q}} \sin \frac{\pi p}{q} \pm \delta e^{\frac{2i\pi p}{q}}, \tag{5.6}$$

and thus (2.6) can be written in the form

$$\left|\delta + O(\delta^2 q) - \frac{1}{q^2}\right| = \frac{1}{q^2}, \tag{5.7}$$

which confirms Mandelbrot's numerical observation (since $\delta^2 q \ll \frac{1}{q^2}$ when $\delta \sim \frac{1}{q^2}$).

Next, Mandelbrot introduces his n^2 conjecture (n is the same as q). This states, in our notation, that for the map F given by (5.2), the derivative with respect to λ along the ray $\lambda \propto \lambda_{p,q} \equiv \exp(2\pi ip/q)$ (thus in the left primary bulb) of the qth iterate gradient $F_q' \equiv \frac{dF_q}{dZ}$, evaluated on the period q orbit which bifurcates at $\lambda_{p,q}$, is equal to $-q^2$. Here F_q is the qth iterate of F. More plainly, in the vicinity of the bulb root $\lambda_{p,q}$,

$$F_q' \approx 1 - q^2\left(\frac{\lambda}{\lambda_{p,q}} - 1\right), \tag{5.8}$$

and this is in fact equivalent to (5.7), since the stability boundary is just $|F_q'| = 1$.

As noted above, Mandelbrot was unable to prove his conjecture, but this was done by Guckenheimer and McGehee [8]. The question then is how their proof relates to our method. There are some points of similarity (for example our result (4.28) is similar to an old result of Fatou), but the tone is quite distinct. In particular, the present calculations give explicit results which are not present in Guckenheimer and McGehee's paper and, although we have not attempted to do so, they provide an entry point for computing higher order approximations.

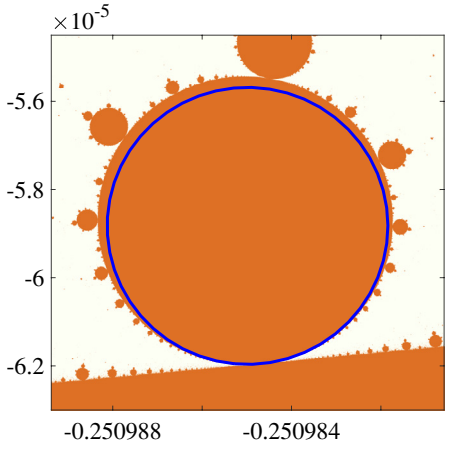

Fig. 4. A close-up of the (1,100) bulb.

Table 1
Analytic and computed values of the bulb radius for various values of p and q. Since the analytic value for 1,2 is exact, its numerical value provides an accuracy check on the numerical algorithm used.

p	q	Analytic	Numerical	Relative error
1	2	0.25	0.250	0.001
1	3	0.0962	0.094	0.02
2	3	0.0962	0.094	0.02
1	11	0.2328×10^{-2}	0.242×10^{-2}	0.04
5	11	0.8180×10^{-2}	0.87×10^{-2}	0.06
1	32	0.9572×10^{-4}	0.996×10^{-4}	0.04
17	32	0.9719×10^{-3}	1.08×10^{-3}	0.10
1	256	0.1872×10^{-6}	0.194×10^{-6}	0.03
129	256	0.1526×10^{-4}	0.168×10^{-4}	0.09
1	1,024	0.2926×10^{-8}	0.300×10^{-8}	0.02
513	1,024	0.9537×10^{-6}	1.039×10^{-6}	0.08

Comparison of the prediction with numerical estimates

The prediction in (5.1) is only an approximation, and as can be seen in Fig. 4, while the estimate is good it is not perfect. In Table 1 we compare analytic estimates given by (5.1) with numerically computed estimates. Since the bulbs are not exact circles, there is some flexibility in defining what an appropriate bulb 'radius' actually is. The method used to here is to estimate bulb area by counting pixels (of size 0.001 relative to the bulb diameter, which is thus the inherent numerical error in estimation of the radius), and computing the equivalent circle radius from that. While we would hope that the relative error would decrease as q increases, it is clear that any such trend, if present at all, is very mild. Improving the approximation provides an intriguing, if perhaps fruitless, direction for future work.

Author contributions

ACF designed the project, carried through the analytic work and wrote the paper. MJM carried out all numerical work and produced all the figures. Both authors produced the final text.

Declaration of Competing Interest

We do not have any conflict of interest.

Acknowledgements

A.C.F. acknowledges the support of the Mathematics Applications Consortium for Science and Industry (http://www.macsi.ul.ie) funded by the Science Foundation Ireland mathematics grant 12/IA/1683.

References

[1] Andreadis I, Karakasidis TE. On a numerical approximation of the boundary structure and of the area of the Mandelbrot set. Nonlinear Dyn 2015;80:929–35.
[2] Blanchard P. Complex analytic dynamics on the Riemann sphere. Bull Amer Math Soc 1984;2:85–141.
[3] Buff X, Epstein AL. A parabolic Pommerenke-Levin-Yoccoz inequality. Fundam Math 2002;172:249–89.
[4] Devaney RL. The Mandelbrot set, the Farey tree, and the Fibonacci sequence. Amer Math Monthly 1999;106(4):289–302.
[5] Devaney RL. The complex geometry of the Mandelbrot set. In: Sanayei A, Zelinka I, Rössler O, editors. ISCS 2013: interdisciplinary symposium on complex systems. emergence, complexity and computation, vol. 8. Berlin: Springer–Verlag; 2014. p. 3–8.
[6] Douady A, Hubbard J. Itération des polynôme quadratiques complexes. C R Acad Sci 1982;294:123–6.
[7] Eckmann J-P, Epstein H. Scaling of Mandelbrot sets generated by critical point preperiodicity. Commun Math Phys 1985;101:283–9.
[8] Guckenheimer J, McGehee R. A proof of the Mandelbrot N^2 conjecture. Institut Mittag-Leffler, Report No. 15; 1984. 12 pp.
[9] Hoppensteadt FC, Miranker WL. Multitime methods for systems of difference equations. Stud Appl Math 1977;56:273–89.
[10] Mandelbrot BB. On the dynamics of iterated maps III: the individual molecules of the M-set, self-similarity properties, the empirical n^2 rule, and the n^2 conjecture. In: Fischer P, Smith WR, editors. Chaos, fractals, and dynamics. New York and Basel: Marcel Dekker; 1985. p. 213–24.
[11] Stephenson J. Formulae for cycles in the Mandelbrot set. Phys A 1991;177:416–20.
[12] Stephenson J. Formulae for cycles in the Mandelbrot set III. Phys A 1992;190:117–29.
[13] Stephenson J, Ridgway DT. Formulae for cycles in the Mandelbrot set II. Phys A 1992;190:104–16.